Lamina Cribrosa and Choroid Features and Their Relationship to Stage of Pseudoexfoliation Glaucoma

Sasan Moghimi,[1,2] Shahbaz Nekoozadeh,[2] Nazgol Motamed-Gorji,[2] Rebecca Chen,[3] Masoud Aghsaei Fard,[2] Massood Mohammadi,[2] and Robert N. Weinreb[1]

[1]Hamilton Glaucoma Center, Shiley Eye Institute, Department of Ophthalmology, University of California, San Diego, California, United States
[2]Tehran University of Medical Sciences, Tehran, Iran
[3]Case Western Reserve University School of Medicine, Cleveland, Ohio, United States

Correspondence: Robert N. Weinreb, Hamilton Glaucoma Center, Department of Ophthalmology, University of California San Diego, La Jolla, CA, USA; rweinreb@ucsd.edu.

Submitted: June 25, 2018
Accepted: September 27, 2018

Citation: Moghimi S, Nekoozadeh S, Motamed-Gorji N, et al. Lamina cribrosa and choroid features and their relationship to stage of pseudoexfoliation glaucoma. *Invest Ophthalmol Vis Sci*. 2018;59:5355–5365. https://doi.org/10.1167/iovs.18-25035

Purpose. To better understand the relationship of lamina cribrosa (LC) and choroid features to the severity of pseudoexfoliation glaucoma (PXG).

Methods. In this cross-sectional study, 137 eyes of 122 subjects (47 eyes with moderate/advanced PXG [mean deviation (MD), −15.0 ± 7.7 dB], 34 eyes with mild PXG [MD, −2.7 ± 1.5 dB], 32 aged-matched pseudoexfoliation syndrome [PXS] eyes, and 24 aged-matched control eyes) were investigated. Optic discs, LC thickness, and anterior LC depth (ALD; midsuperior, center, and midinferior) as well as peripapillary choroidal thickness were determined. Linear mixed modeling was used to adjust for age, sex, and axial length.

Results. A progressive decrease in LC thickness was found when comparing controls (271.9 ± 61.3 μm), PXS (212.6 ± 51.5 μm), mild PXG (180.8 ± 24.6 μm), and moderate/advance PXG (138.9 ± 37.5 μm) ($P < 0.001$). ALD was greater ($P < 0.001$) in moderate/advance glaucoma (306.7 ± 105.3 μm) and mild PXG (209.5 ± 79.7 μm) compared with PXS (155 ± 86.7 μm) and healthy controls (149.2 ± 103 μm). Although eyes with moderate/advance PXG had the thinnest choroid (117.2 ± 36.6 μm), choroidal thickness was comparable in mild PXG, PXS, and controls (150.0 ± 46.1, 159.7 ± 65.5, and 157.5 ± 51.1 μm, respectively; $P = 0.002$). Worse MD was the only factor associated with thinner LC ($\beta = 2.344$, $P < 0.001$) and choroid ($\beta = 1.717$, $P = 0.009$ μm) in PXG eyes. Higher IOP ($\beta = 4.305$, $P = 0.013$) and worse MD ($\beta = -6.390$, $P < 0.001$) were associated with deeper ALD in PXG.

Conclusions. In pseudoexfoliation, LC thinning is an early sign, and there is progressive thinning with advancing glaucoma. Choroidal thinning is observable only with moderate/advanced glaucoma. In PXG eyes, LC thickness, depth, and peripapillary choroidal thickness are associated with glaucoma severity.

Keywords: pseudoexfoliation, glaucoma, lamina cribrosa, choroid

Pseudoexfoliation syndrome (PXS) is an age-dependent disorder characterized by abnormal elastosis and deposition of microfibril material throughout extracellular matrix systemically, including in ocular tissue. PXS is the most recognized independent risk factor for glaucoma, as approximately half of patients develop secondary open angle glaucoma (OAG) during their lifetime, and pseudoexfoliation glaucoma (PXG) globally accounts for 25% of OAG cases.[1] Deposition of pseudoexfoliative material in the trabecular meshwork and blockade of Schlemm's canal consequently results in IOP elevation and development of PXG. In comparison to POAG, PXG is associated with higher IOP and greater IOP fluctuation. Patients with PXG more commonly experience failure of medical management, and overall they are predisposed to faster progression and a poorer prognosis.[2–4] Although the role of high IOP in PXG has been widely recognized, it has been suggested that the probability of developing glaucomatous damage at a given IOP is higher in PXS compared with healthy controls.[3] Therefore, it is suspected that PXS vulnerability toward glaucoma may be partially attributed to IOP-independent factors.[1–5]

Several studies have suggested the lamina cribrosa (LC) to be one of the structures affected by abnormal elastosis in PXS.[6–8] The LC is a mesh-like structure located at the scleral level, consisting of collagen beams and pores through which optic nerve axons traverse, and it is recognized as the primary site of ganglion cell axonal injury in glaucoma.[9] Previous studies have discussed the association of LC thinning and its displacement with the existence of glaucoma, including POAG and normal tension glaucoma (NTG). Findings of these studies suggest that a defective LC structure could primarily result in glaucomatous optic neuropathy, despite a normal or controlled IOP.[9–11] Previous studies also have reported LC alterations in early stages of PXS without glaucoma and, similarly, PXG is associated with thinner LC compared with POAG. Overall, it has been suggested that the elastotic abnormality of the LC in PXS could result in decreased stiffness and increased deformability, thereby placing patients at risk of developing glaucomatous optic neuropathy.[7,12–14] However, the causality of this association has not been established thus far.

Many studies have addressed the role of choroidal blood supply in the development of glaucoma.[15–21] Although the

posterior ciliary arteries supply most of the laminar region of optic nerve head (ONH), the prelaminar region and surface of optic disc are primarily supplied by the peripapillary choroid.[22] Therefore, choroidal circulation has been suggested to contribute to the pathophysiology of glaucomatous optic neuropathy. Findings regarding choroidal involvement in glaucoma (reflected as choroid thickness) have been discrepant, as several studies reported thinning of the macular or peripapillary choroid in patients with POAG or NTG,[23,24] while other studies have failed to find a difference in choroidal thickness in glaucoma as compared with healthy subjects.[21,25]

Most of these studies have focused on choroid and LC changes in POAG, and a limited number of investigations have focused on the changes in LC and choroidal variations in the full spectrum of the pseudoexfoliation. Further, factors correlated with choroidal and LC structures in PXG have not been evaluated. Therefore, the nature of association between choroidal thickness, LC, and PXG remains unclear. Choroidal involvement has been a controversial factor in development of glaucoma in PXS with. There are conflicting results from several studies describing thinner choroid in PXS and PXG[26–28] and other studies that did not find a difference.[12,29,30]

Spectral-domain optical coherence tomography (SD-OCT) is an imaging modality that provides a noninvasive cross-sectional view of the posterior segment of the eye and is widely used for in vivo evaluation of ONH structures in glaucoma.[31] Enhanced-depth imaging (EDI) SD-OCT has been used for evaluating the deeper structures of the ONH and choroid by many investigators.[9,11–13,29,30,32,33] The current study aimed to evaluate LC features and peripapillary choroidal thickness in PXS patients (with and without glaucoma) using EDI SD-OCT and to identify factors affecting choroidal thickness and LC in these patients.

Materials and Methods

Patients

This is a case-control cross-sectional study conducted from September 2013 to September 2017 at Farabi Eye Hospital in Tehran, Iran. Three groups of subjects were investigated in this study as follows: (1) pseudoexfoliation eyes with glaucoma ("PXG" group), (2) age-matched PXS eyes without glaucoma ("PXS" group), and (3) age-matched healthy volunteers ("control" group). Controls were selected among individuals who were referred to the hospital for routine and/or refractive check-ups. A complete ophthalmic examination was performed for all subjects, including best-corrected visual acuity measurement (using the Early Treatment Diabetic Retinopathy Study chart), slit-lamp biomicroscopy, Goldmann applanation tonometry, gonioscopy, dilated stereoscopic fundus examination using a 90- or 78-diopter (D) lens, measurement of the central corneal thickness by pachymetry (Tomey Corporation, Nagoya, Japan), visual field test (Humphrey Field Analyzer II 750; 24-2 Swedish interactive threshold algorithm; Carl Zeiss Meditec, Dublin, CA, USA), axial length measurement (IOL-Master; Carl Zeiss Meditec), and SD-OCT imaging of the ONH and macula (Spectralis OCT; Heidelberg Engineering, Inc., Dossenheim, Germany).

For all study participants, inclusion criteria were as follows: (1) age above 18 years; (2) best-corrected visual acuity of 0.5 logMAR or better with a spherical equivalent within 5 D and a cylinder correction within 3 D; and (3) reliable Humphrey Field Analyzer results with a false-positive error rate less than 15%, a false-negative error rate less than 20%, and a fixation loss rate less than 20%. The exclusion criteria were as follows: (1) presence of other intraocular or neurologic disorder that could cause visual field impairment; (2) history of any ocular surgery; (3) a diagnosis of glaucoma in the fellow eye; (4) hazy media interfering with OCT imaging; or (5) history of diabetes mellitus.

Patients were enrolled in the PXG group if they had (1) pseudoexfoliation material on the anterior lens capsule and/or pupillary margin after mydriasis on slit-lamp biomicroscopy; (2) glaucomatous optic neuropathy (thinning or notching of the neural rim); (3) glaucomatous visual field defect defined as a Glaucoma Hemifield Test outside of normal limits and four abnormal points with $P < 5\%$ on the pattern deviation plot, both confirmed at least once on 24-2 visual fields[34]; and (4) history of IOP greater than 21 mm Hg without treatment. The PXS group were defined as (1) visible pseudoexfoliation material on the anterior lens capsule and/or pupillary margin after mydriasis on slit-lamp biomicroscopy; (2) IOP less than 22 mm Hg without treatment; (3) negative history of elevated IOP; (4) absence of glaucomatous disc appearance (i.e., intact neuroretinal rim without cupping, notches, or localized pallor); and (5) a normal standard automated perimetry defined by mean deviation (MD) and pattern standard deviation (PSD) within 95% CI limits and a Glaucoma Hemifield Test within normal limits. The control group was defined as (1) IOP less than 22 mm Hg without treatment; (2) negative history of elevated IOP; (3) absence of glaucomatous disc appearance; (4) normal standard automated perimetry; and (5) absence of pseudoexfoliation material on the anterior lens capsule or pupillary margin after mydriasis on slit-lamp biomicroscopy in both eyes.

This study was approved by the local Ethical Committee of Tehran University of Medical Sciences and was conducted in accordance with the Declaration of Helsinki. All patients provided written informed consent prior to enrollment in the study.

Spectral-Domain Optical Coherence Tomography

Optic Nerve Head Measurements. All study participants underwent SD-OCT imaging. Measurements were performed after pupillary dilation, using SD-OCT (Heidelberg Spectralis SD-OCT; Spectralis software version 5.3.2; Heidelberg Engineering, Inc.). The EDI-OCT technique in ONH has been described in previous publications.[35] In brief, the SD-OCT device was set to scan a $15° \times 10°$ rectangle centered on the ONH. This rectangle was divided into approximately 65 horizontal sections, each of which had an average of 42 OCT frames. Three sections that passed through the ONH in the center, midsuperior, and midinferior regions ("Cen," "Sup," and "Inf," respectively) were selected, and all study parameters were measured in each of these frames. To overcome the effect of choroidal thickness on LC depth measurements, the sclerochoroid junction reference plane was used for ONH measurements.[36] Figure 1 depicts the LC surfaces and the sclerochoroidal border in an ONH OCT image. The sclerochoroid junction reference line was defined as the line connecting two points of the anterior scleral surface located at 1750 μm from the center of the Bruch's membrane opening (BMO) in each B scan. All measurements were made perpendicular to the reference line. Parameters were measured as close as possible to the vertical center of the ONH. In cases where the central retinal vessel trunk prevented visualization, measurements were performed on the temporal side. The anterior and posterior margins of the highly reflective region at ONH vertical center in the horizontal SD-OCT cross-section were used as the borders of the LC, and the perpendicular distance between these borders was identified as LC thickness. The prelaminar thickness was defined as the distance between the anterior surface of the optic cup and the anterior border of the

Investigative Ophthalmology & Visual Science

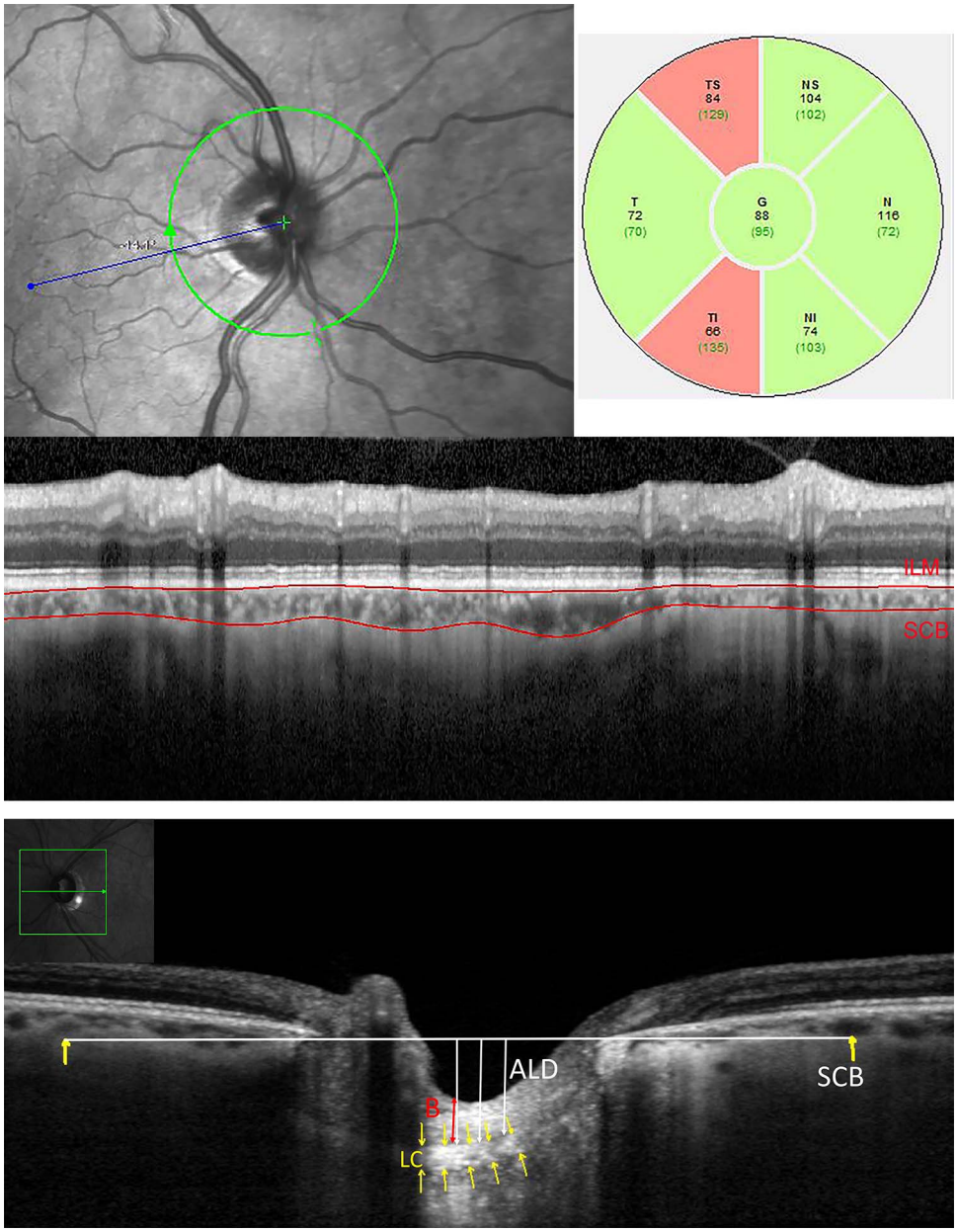

Figure 1. *Top*: a peripapillary OCT circular scan depicts the manual segmentation of Bruch's membrane (*upper red line*) and sclerochoroidal border (*lower red line*) and global thickness of peripapillary choroid as well as six sectors of Heidelberg layout. *Bottom:* an EDI-OCT of optic nerve head shows sclerochoroidal border (SCB) and the reference line, anterior and posterior border of LC (*yellow arrows*), ALD (*white arrows*), and prelaminar thickness (*B*, *red arrow*) in a raster line across the center of optic nerve.

LC, and the anterior LC depth (ALD) was defined as the perpendicular distance from the anterior LC surface to the sclero-choroidal junction (SCJ) line. In a single central B scan, all the measurements were taken at the following three points: the maximally depressed point of the anterior surface of LC and two additional points at 100 and 200 μm temporally from the maximally depressed point. Only the temporally adjacent points were selected. The mean of the three measurements was used for analysis.[37] All of the measurements were performed using HEYEX software 6.0 (Heidelberg Engineering, Inc.) and analyzed by two masked specialists in two different sessions.

Choroid Thickness Measurement. According to the standard protocol for retinal nerve fiber layer (RNFL) assessment, a 360° circular scan pattern with 3.4-mm diameter was used for measuring peripapillary choroidal thickness and peripapillary RNFL.[38] The upper and lower segmentation lines of the circular scan were manually delineated in order to assess peripapillary choroid thickness. The lines were adjusted to align with the inner scleral wall and posterior border of the RPE to define the outer and inner boundaries of the choroid, respectively. The choroidal thickness in the investigated sectors was automatically computed using the RNFL thickness sectors algorithm (Fig. 1).

Twenty randomly selected EDI-OCT B scans from 20 eyes were used to assess the intraobserver and interobserver reproducibility of LC and choroidal thickness measurements. This analysis was based on two independent series of re-evaluations performed by two independent examiners. The absolute agreement of a single observer's measurements and

Table 1. Clinical and Demographic Characteristics of PXG, PXS, and Control Group

	PXG Group ($n = 81$)	PXS Group ($n = 32$)	Control Group ($n = 24$)	P*	$P1$†	$P2$†	$P3$†
Age, y	70.4 ± 7.7	69.6 ± 7	66.7 ± 6.3	0.145	0.678	0.085	0.678
Sex (female/male)	18/63	13/19	13/11	**0.007**	–	–	–
SE, D	−0.70 ± 2.05	−0.91 ± 2.02	−0.83 ± 1.21	0.916	0.697	0.791	0.893
IOP at presentation, mm Hg	17.2 ± 8.1	15.3 ± 2.3	13.9 ± 2.3	**0.005**	0.079	**0.002**	**0.041**
IOP at OCT examination, mm Hg	16.3 ± 5.3	15.3 ± 2.3	13.9 ± 2.3	**0.011**	0.248	**0.004**	**0.041**
CCT, μm	520.5 ± 29.4	518.3 ± 28.8	539.6 ± 40.2	0.208	0.779	0.115	0.083
Axial length, mm	23.1 ± 0.76	22.8 ± 0.76	23.3 ± 0.73	0.720	0.401	0.532	0.730
Visual field MD, dB	−10.1 ± 8.7	−0.1 ± 1.4	−0.25 ± 1.37	**<0.001**	**<0.001**	**<0.001**	0.694
RNFL, μm							
Superotemporal, μm	88.7 ± 33.3	121.5 ± 19.7	125.0 ± 15.5	**<0.001**	**<0.001**	**<0.001**	0.583
Superonasal, μm	78.3 ± 27.6	103.2 ± 18.6	109.1 ± 22.9	**<0.001**	**<0.001**	**<0.001**	0.396
Nasal, μm	57.0 ± 19.4	77.0 ± 9.7	77.8 ± 11.8	**<0.001**	**<0.001**	**<0.001**	0.816
Inferonasal, μm	84.8 ± 31.7	121.2 ± 21.5	119.2 ± 24.2	**<0.001**	**<0.001**	**<0.001**	0.792
Inferotemporal, μm	88.4 ± 36.1	118.5 ± 28.8	136.6 ± 20.0	**<0.001**	**<0.001**	**<0.001**	**0.046**
Temporal, μm	56.0 ± 16.1	61.8 ± 13.3	61.3 ± 12.7	0.155	0.140	0.107	0.912
Global, μm	70.5 ± 20.7	92.2 ± 13.3	96.1 ± 11.5	**<0.001**	**<0.001**	**<0.001**	0.230

* Linear mixed model.

† $P1$: Pairwise comparison between PXG and PXS groups; $P2$: pairwise comparison between PXG and control groups, pairwise comparison between PXS and control groups. The disease status was used as a nominal parameter in the model. P values <0.05 are shown in bold.

the mean of the measurements conducted by two observers were estimated using the intraclass correlation coefficient (ICC) via a two-way mixed-effect model. ICC scores 0.75 or more, 0.40 to 0.75, and 0.4 or less were considered excellent, moderate, and poor, respectively.[39] Scans with quality scores below 15 were excluded from the analysis. Scans with inadequate quality as determined by obscured images of fundus, RNFL interruption, or unclear border of the LC or posterior choroid were excluded as well.

Statistical Analysis

Continuous variables were reported as mean and SD. Comparisons between the groups were performed using a linear mixed model accounting for intereye correlation. The disease status was used as a nominal parameter in the model, and the results were reported before and after adjustment for age, sex, and axial length. In order to evaluate factors associated with LC/choroid parameters in PXG patients, a model was built with choroidal and LC thickness as outcome variables, and variables associated with LC or choroidal parameters in univariate analysis were reported. A multivariate model was also designed for LC and choroidal parameters including age, sex, and variables with both P less than 0.20 in univariate analysis and variance inflation factor (VIF) less than 3 (to exclude collinearity). An interaction term between age and PXG status was also fitted in a model to explore if the relationship between LC/choroid parameters and age was influenced by disease status. Statistical analyses were performed using statistical software Stata 14.2 (StataCorp LLC, College Station, TX, USA). P values less than 0.05 were considered statistically significant.

Results

The current study included 81 eyes of 71 PXG patients, 32 eyes of 28 PXS patients, and 24 eyes of 23 control subjects. Table 1 depicts the demographics and baseline characteristics of the participants. The mean age was comparable among the 3 groups (70.4 ± 7.7 vs. 69.6 ± 7, vs. 66.7 ± 6.3 year for PXG, PXS and control, respectively; $P = 0.145$). Although there was a higher proportion of women in the control group ($P = 0.007$), the three groups were comparable in regard to axial length ($P = 0.720$) and CCT ($P = 0.208$). Compared with PXG and PXS eyes, control eyes had significantly lower IOPs ($P = 0.002$ and $P = 0.041$, respectively). PXG eyes had worse MD ($P < 0.001$) and RNFL thickness globally ($P < 0.001$) and in each sector (except the temporal sector). Intraobserver and interobserver reproducibility of ONH and peripapillary choroid parameters were excellent and ranged from 0.943 to 0.998 for choroidal measurements and from 0.827 to 0.998 for ONH measurements.

ONH and LC measurements are demonstrated in Table 2. All three groups had comparable BMO area (adjusted $P = 0.174$) However, there were significant differences in central LC thickness, which was thinnest in PXG eyes (155.7 ± 38.7 μm), followed by PXS eyes (212.6 ± 51.5 μm) and then controls eyes (271.9 ± 61.3 μm) (adjusted $P < 0.001$, $P \leq 0.001$ for all pairwise comparisons). Similarly, inferior and superior LC thicknesses were thinnest in PXG eyes, followed by PXS eyes and controls (adjusted $P < 0.001$; $P \leq 0.001$ for all pairwise comparisons). PXG eyes had deeper ALD than PXS (adjusted $P < 0.001$) and control eyes (adjusted $P = 0.001$) in all regions. However, no significant difference in ALD was observed between PXS and controls (adjusted $P > 0.397$ for all regions).

Table 2 shows the peripapillary choroidal thickness among the three groups. Global peripapillary choroidal thickness was significantly thinner (131 ± 43.7 μm) in PXG eyes than in PXS (159.7 ± 65.5 μm) and control eyes (157.5 ± 51.1 μm) (adjusted $P = 0.039$). Similar results were found for all the sectors except the supratemporal, supranasal, and nasal sectors. PXS and control eyes had comparable choroidal thickness globally and in all sectors (adjusted $P \leq 0.015$).

Table 3 presents the results of subgroup analysis in PXG eyes. Age, sex, spherical equivalent (SE), IOP, and axial length were comparable between mild PXG and moderate/advanced PXG ($P > 0.161$ for all). There were statistically significant differences in standard structural and functional measurements between the groups ($P < 0.001$). Central, inferior, and superior LC thicknesses were thinner in the moderate/advanced PXG eyes (138.9 ± 37.5, 138.2 ± 35.8, and 134.9 ± 36.3 μm, respectively) compared with mild PXG eyes (180.8 ± 24.6, 166.5 ± 31.3, and 165.6 ± 24.5 μm, respectively) (adjusted $P < 0.001$ for all the regions). Likewise, moderate/advanced PXG had deeper ALD compared with mild PXG in all regions

Investigative Ophthalmology & Visual Science

Table 2. Comparison of Peripapillary Choroidal Thickness and ONH Structures Among Eyes PXG, PXS, and Control Group

Location	PXG Group (n = 81)	PXS group (n = 32)	Control Group (n = 24)	P^* (P')‡	$P1$† ($P1'$)‡	$P2$† ($P2'$)‡	$P3$† ($P3'$)‡
ONH structures							
BMO, µm§	1548.7 ± 155.6	1543.2 ± 183.2	1500.9 ± 190.4	0.571 (0.174)	0.898 (0.425)	0.294 (0.504)	0.445 (0.130)
$_{Cen}$ Prelaminar thickness, µm	177.5 ± 118	233.9 ± 134.8	241.6 ± 156.1	0.054 (0.168)	0.067 (0.178)	**0.044** (0.112)	0.837 (0.827)
$_{Cen}$ ALD, µm	267.8 ± 106.6	155 ± 86.7	149.2 ± 103	**<0.001** (<0.001)	**<0.001** (<0.001)	**<0.001** (<0.001)	0.845 (0.762)
$_{Cen}$ LC thickness, µm	155.7 ± 38.7	212.6 ± 51.5	271.9 ± 61.3	**<0.001** (<0.001)	**<0.001** (<0.001)	**<0.001** (<0.001)	**0.001** (0.002)
$_{sup}$ ALD, µm	316 ± 108.9	202.4 ± 79.7	177.3 ± 102.8	**<0.001** (<0.001)	**<0.001** (<0.001)	**<0.001** (0.001)	0.469 (0.507)
$_{Sup}$ LC thickness, µm	149.3 ± 36.6	181.2 ± 49.7	264.1 ± 102.8	**<0.001** (0.001)	**0.021** (0.210)	**<0.001** (<0.001)	**0.012** (0.007)
$_{Inf}$ ALD, µm	269.4 ± 101.9	155.6 ± 74.3	109.3 ± 115.6	**<0.001** (<0.001)	**0.001** (<0.001)	**0.001** (0.002)	0.340 (0.397)
$_{Inf}$ LC thickness, µm	147.7 ± 35.1	181.1 ± 32.6	258.5 ± 61	**<0.001** (<0.001)	**<0.001** (0.001)	**<0.001** (<0.001)	**0.001** (0.001)
Choroidal thickness							
Superotemporal, µm	145.6 ± 48.5	164.4 ± 73.9	175.5 ± 57	0.055 (0.265)	0.208 (0.226)	**0.024** (0.060)	0.534 (0.635)
Superonasal, µm	145.5 ± 51.4	159.6 ± 66.2	172.5 ± 50.9	0.096 (0.161)	0.332 (0.380)	**0.038** (0.066)	0.466 (0.522)
Nasal, µm	135.4 ± 55.0	158.6 ± 69.9	162.9 ± 56.4	0.079 (0.109)	0.144 (0.159)	**0.049** (0.069)	0.819 (0.856)
Inferonasal, µm	106.3 ± 44.2	144 ± 69.4	140 ± 58.2	**0.002** (0.005)	**0.008** (0.010)	**0.007** (0.014)	0.809 (0.745)
Inferotemporal, µm	107.6 ± 50.6	148.6 ± 62	133.7 ± 50.6	**0.001** (0.009)	**0.049** (0.073)	0.003 (0.003)	0.549 (0.659)
Temporal, µm	136 ± 47.2	170.3 ± 70.5	159.5 ± 54	**0.022** (0.046)	**0.017** (0.024)	0.064 (0.140)	0.611 (0.426)
Global, µm	131 ± 43.7	159.7 ± 65.5	157.5 ± 51.1	**0.019 (0.039)**	**0.033** (0.043)	**0.026** (0.051)	0.893 (0.179)

* Linear mixed model.

† P1: pairwise comparison between PXG and PXS groups; P2: pairwise comparison between PXG and control groups, pairwise comparison between PXS and control groups. The disease status was used as a nominal parameter in the model.

‡ Adjusted for age, sex, IOP, and axial length. P values <0.05 are shown in bold.

Table 3. Comparison of Clinical and Demographic Characteristics, ONH Measurements, and Choroidal Thickness in Different Peripapillary Locations in PXG Eyes According to Severity of Glaucoma

	Moderate/Advanced PXG ($n = 47$)	Mild PXG ($n = 34$)	P*	Adjusted P†
Age, y	69.9 ± 7	71 ± 8.6	0.552	-
Sex (female/male)	10/37	8/26	0.810	-
SE, D	−0.85 ± 1.89	−0.50 ± 2.27	0.559	-
IOP at presentation, mm Hg	17.3 ± 9.2	17.2 ± 6.3	0.976	-
IOP at OCT examination, mm Hg	16.1 ± 5.7	16.6 ± 4.7	0.672	
CCT, µm	514.5 ± 27.3	528.6 ± 31.1	0.161	-
Axial length, mm	23.13 ± 0.77	23.27 ± 0.75	0.473	-
Visual field MD (dB)	−15.0 ± 7.7	−2.7 ± 1.5	**<0.001**	-
Global RNFL, µm	57.9 ± 14.9	87.6 ± 13.8	**<0.001**	-
ONH structure				
BMO, µm	1546.1 ± 157.3	1552.9 ± 156	0.864	0.836
$_{Cen}$ Prelaminar thickness, µm	163.1 ± 101.6	199.6 ± 138.7	0.296	0.202
$_{Cen}$ ALD, µm	306.7 ± 105.3	209.5 ± 79.7	**<0.001**	**<0.001**
$_{Cen}$ LC thickness, µm	138.9 ± 37.5	180.8 ± 24.6	**<0.001**	**<0.001**
$_{Sup}$ ALD, µm	349.5 ± 115.1	263.7 ± 74.1	**0.001**	**0.001**
$_{Sup}$ LC thickness, µm	138.2 ± 35.8	166.5 ± 31.3	**0.002**	**0.008**
$_{Inf}$ ALD, µm	294.9 ± 105.7	233.1 ± 85.4	**0.016**	**0.010**
$_{Inf}$ LC thickness, µm	134.9 ± 36.3	165.6 ± 24.5	**<0.001**	**0.001**
Choroidal thickness				
Superotemporal, µm	134.6 ± 47.1	160.3 ± 47.3	**0.026**	**0.015**
Superonasal, µm	131.2 ± 42.7	164.2 ± 56.4	**0.010**	**0.005**
Nasal, µm	116.8 ± 39.3	160.1 ± 63.2	**0.003**	**0.001**
Inferonasal, µm	91.7 ± 37.0	125.7 ± 46.2	**0.003**	**<0.001**
Inferotemporal, µm	95.2 ± 33.5	123.6 ± 43.4	**0.003**	**0.001**
Temporal, µm	124.4 ± 45.1	151.4 ± 46.2	**0.014**	**0.004**
Global, µm	117.2 ± 36.6	150.0 ± 46.1	**0.003**	**0.003**

* Linear mixed model. The disease status was used as a nominal parameter in the model.
† Adjusted for age, sex, IOP, and axial length. P values <0.05 are shown in bold.

(adjusted $P < 0.010$ for all regions). Moderate/advanced PXG eyes had thinner peripapillary choroid than mild PXG eyes globally and in each sector (adjusted $P < 0.001$ for all regions).

Overall, central LC thickness progressively decreased from controls to PXS to mild PXG to moderate/advance PXG (adjusted $P < 0.001$). ALD was deeper in moderate/advanced and mild PXG eyes compared with PXS and healthy controls (adjusted $P < 0.001$). Although moderate/advanced PXG eyes had the thinnest choroid, choroidal thickness was comparable in mild PXG, PXS, and control eyes (adjusted $P = 0.002$) (Fig. 2).

Factors associated with laminar and choroidal measurements in PXG eyes in univariate and multivariate analyses are demonstrated in Table 4 and Figure 3. RNFL (VIF > 3) was not included in the multivariable analysis to reduce collinearity in the final model. Older age, worse MD, and thinner RNFL were associated with thinner LC thickness in univariate analysis. In multivariate analysis, only worse MD was associated with thinner LC ($\beta = 2.344$, $P < 0.001$). Factors associated with deeper central ALD in univariate analysis included thinner RNFL and worse MD. When fitted in a multivariate model, higher IOP ($\beta = 4.305$, $P = 0.013$) and worse MD ($\beta = -6.390$, $P < 0.001$) were associated with deeper ALD in PXG eyes. Worse MD was the only factor associated with thinner choroid in both univariate and multivariate ($\beta = 1.717$, $P = 0.009$) analyses.

We also explored whether the relationships between LC thickness, ALD, or choroidal thickness and age were influenced by disease status. Older age was associated with thinner LC ($P = 0.040$), and the relationship between age and LC thickness was not affected by disease status ($P = 0.873$). No link was found between age and ALD in PXG eyes ($P = 0.500$), and PXG status had no influence on the association between ALD and age ($P = 0.124$). Older age was not associated with thinner choroid in PXG eyes ($\beta = -1.09$ µm/y, $P = 0.080$), and these eyes had a lower rate of choroidal thinning each year ($P = 0.046$) compared with control eyes ($\beta = -3.72$ µm/y, $P = 0.002$).

Discussion

In this in vivo human study, we demonstrated a stepwise increase in LC thickness and stepwise decrease in LC depth from controls to PXS to mild PXG to advanced PXG. Although the peripapillary choroid was thinner in moderate/advance PXG, the other groups of mild PXG, PXS, and controls had comparable choroidal thickness. In PXG eyes, LC thickness, depth, and peripapillary choroidal thickness were associated with glaucoma severity.

Deformation and displacement of the LC have been implicated as the primary pathophysiologic mechanism of glaucomatous optic neuropathy.[9–11] The thinning of the LC in various types of glaucoma has been documented in previous reports.[9,11–13,32,33] In a study by Park and associates,[40] LC was thinner in the NTG group than in the POAG and control groups. In their study comparing LC thickness in glaucomatous patients, Kim et al.[13] observed that despite similar mean IOP, the LC was significantly thinner in PXG than POAG. In our previous report, the LC was significantly thinner in non-glaucomatous PXS patients than in controls. In the present study, LC was thinnest in moderate to advanced glaucoma, followed by mild glaucoma, then PXS, and then healthy controls. Our results suggest that LC changes can occur in pseudoexfoliatives eye even before IOP elevation, as eyes with IOP greater than 21 mm Hg were excluded from PXS group in our study.

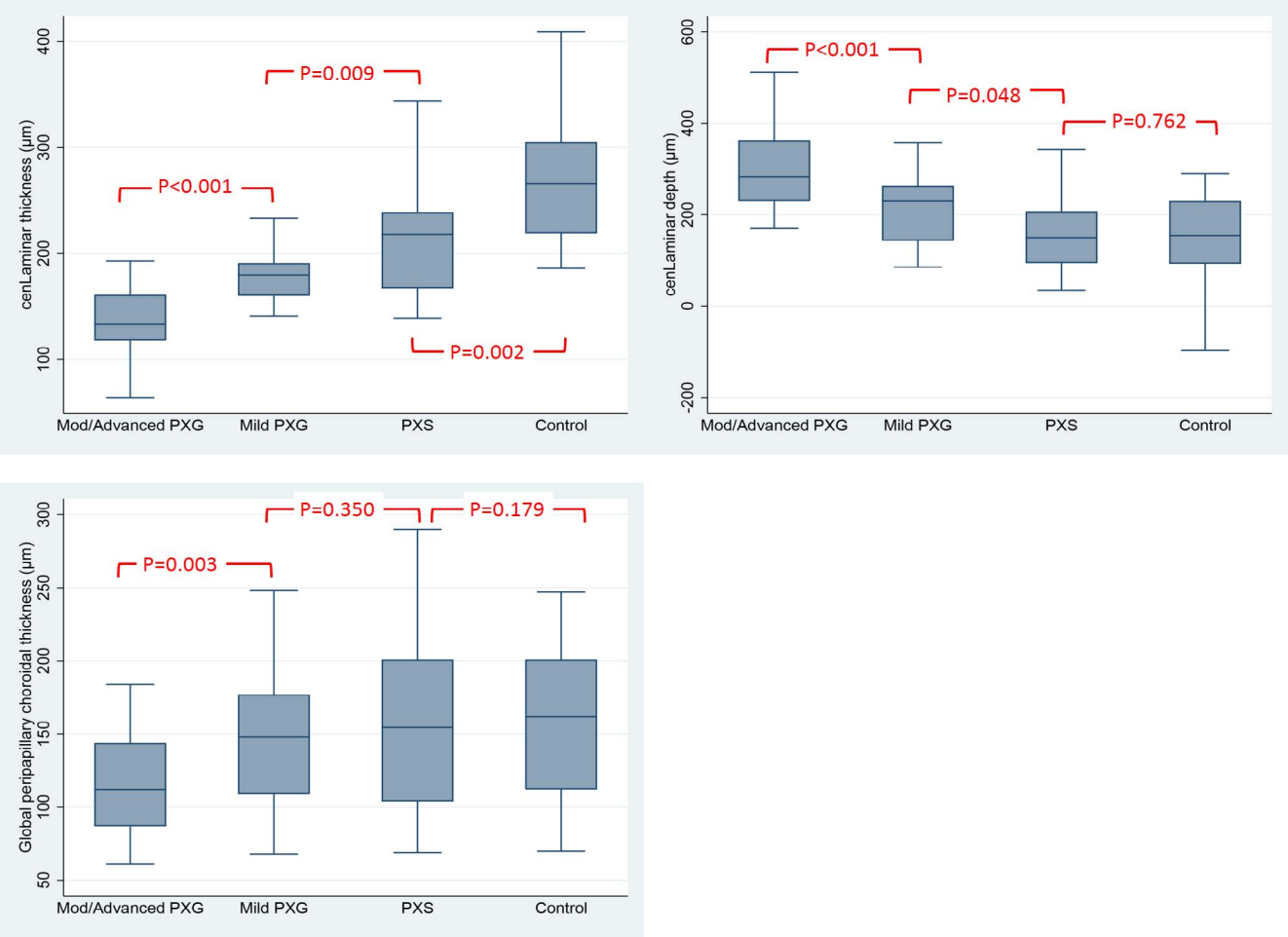

Figure 2. Distribution of central LC thickness (*top left*), central LC depth (*top right*), and, global choroidal thickness (*bottom left*), in four eye groups (moderate/advanced PXG, mild PXG, PXS, and healthy controls) assessed by OCT. Adjusted *P* values for pairwise comparison are provided.

Generalized ultrastructural alterations in ocular tissues and other organs in patients with pseudoexfoliation have been previously demonstrated.[41] Significant downregulation of lysyl oxidase-like 1 and elastic fiber in LC tissues in PXS eyes (without and with glaucoma) compared with normal and POAG specimens has been shown in vitro.[7] These alterations may lead to reduced elasticity of the LC[14] and may place PXS patients at higher risk of glaucomatous damage. Thinning of the LC, besides being a consequence of glaucomatous damage, could also have prognostic and mechanistic significance and may predispose the eye to faster glaucomatous progression.[42] Lee and associates,[42] in a recent study on POAG eyes, demonstrated that a thinner LC is associated with a faster rate of RNFL thinning. A thinner LC may be the result of LC compression, interindividual variation, or both; whichever the case, the thinner LC may affect disease progression.

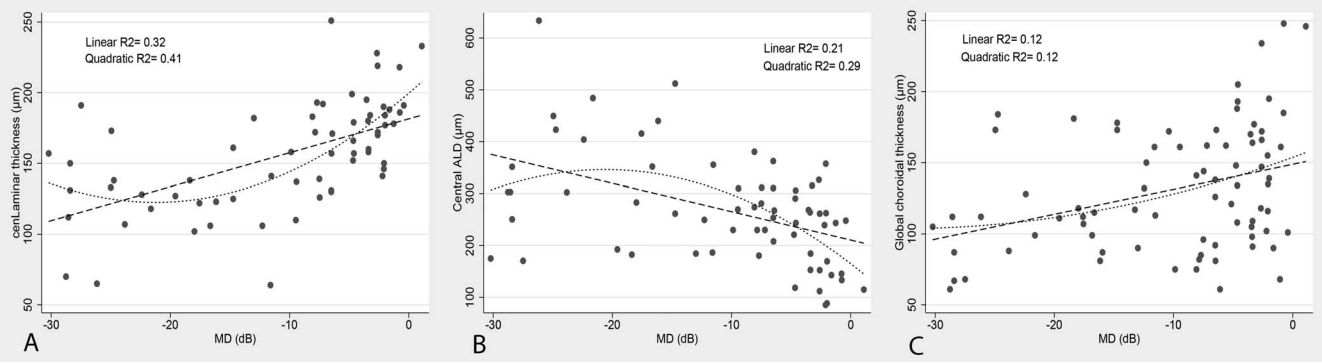

Figure 3. The scatterplots demonstrating the association between central laminar thickness and MD (*right*), the association between central laminar depth and MD (*middle*), and the association between global choroidal thickness and MD (*left*) in eyes with PXG. Linear and quadratic R^2 for the models are provided.

TABLE 4. Factors Associated With Laminar and Choroidal Parameters in PXG Patients

	Central LC Thickness				Central ALD				Global Peripapillary Choroidal Thickness			
	Univariate		Multivariate		Univariate		Multivariate		Univariate		Multivariate	
	β (SE)	*P*	β (SE)	*P*	β (SE)	*P*	β (SE)	*P*	β (SE)	*P*	β (SE)	*P*
Age	−1.044 (0.495)	**0.039**	−0.494 (0.406)	0.229	−1.472 (2.150)	0.496	−2.121 (1.976)	0.288	−1.093 (0.609)	0.077	−0.833 (0.609)	0.176
Sex (male/female)	2.762 (11.058)	0.804	9.238 (9.223)	0.356	0.520 (23.637)	0.983	−35.337 (19.020)	0.069	6.266 (10.858)	0.566	9.977 (11.128)	0.313
Axial length	0.324 (5.235)	0.951	-	-	−3.849 (1.913)	0.060	−11.733 (17.605)	0.508	−3.225 (7.505)	0.669	-	-
CCT	0.094 (0.206)	0.650	-	-	−12.123 (18.491)	0.515			0.499 (0.340)	0.153	-	-
IOP at presentation	−1.005 (0.563)	0.080	−0.452 (0.561)	0.424	0.495 (0.661)	0.161	4.305 (1.686)	**0.013**	−0.524 (0.460)	0.259	-	-
IOP at OCT examination	−1.333 (0.834)	0.117	-	-	0.587 (0.781)	0.210	-	-	−0.409 (0.867)	0.642	-	-
MD	2.396 (0.554)	**<0.001**	2.344 (0.522)	**<0.001**	−5.461 (1.943)	**0.007**	−6.390 (1.557)	**<0.001**	1.751 (0.593)	**0.004**	1.717 (0.635)	**0.009**
Global RNFL	0.914 (0.223)	**<0.001**	-	-	−2.149 (0.751)	**0.004**	-	-	0.719 (0.265)	**0.009**	-	-
BMO area	0.003 (0.024)	0.898	-	-	0.893 (0.085)	0.301	-	-	0.30 (0.041)	0.466	-	-

P values <0.05 are shown in bold.

The association between LC thickness and glaucoma severity differed depending on the type of glaucoma. Park et al.[40] also reported a logarithmic correlation between LC thickness and retinal sensitivity in POAG eyes. Similarly, a small but significant correlation between glaucoma severity (represented by MD) and LC thickness and depth were found by Kim et al.[33] using EDI SD-OCT. Although LC thickness was correlated with MD in the POAG group, the NTG group did not show a significant correlation with disease severity. The investigators proposed that the structural properties of the LC might be different between NTG and high-tension glaucoma eyes. In the current study, we found that LC thickness decreased with disease progression in PXG, similar to in POAG. In this study, age was associated with LC thickness in univariate but not multivariate analysis.

In the current study, PXG eyes had deeper ALD compared with PXS and healthy controls. Deepening of the anterior LC surface has been well documented in glaucomatous eyes and is considered to be the principal pathogenic event leading to axonal damage.[11,33,42,43] This event may cause a blockade of axoplasmic flow by kinking and pinching the retinal ganglion cell axons passing through it, thereby provoking glaucomatous optic nerve damage.[43] Deeper LC has been linked to more rapid glaucomatous damage in a recent study.[42]

Several factors have been reported to be associated with the status and the magnitude of the LC deformation in POAG, including age,[44,45] IOP,[46,47] disease severity,[10,33,45] and phenotype of the glaucomatous disc.[48] However, no study has reported the factors related to LC depth in PXG thus far. In POAG eyes, age appears to be one associated factor,[44,45] as older eyes have less LC deformation than younger eyes for the same level of functional loss. Investigators attributed that difference to changes in the elasticity of lamina and to different responses of lamina to IOP in older individuals. In the present study, no link was found between age and ALD in PXG eyes. The characteristic changes in the LC may occur at younger ages in pseudoexfoliative patients, which could explain the lack of association between age and ALD in PXG.

Another factor is disease severity, in which greater LC deepening is observed in more advanced glaucoma.[49] A recent report by Ren et al.[45] showed an association between the ALD and MD in early glaucoma or ocular hypertension patients. However, in their study, the LC depth increased with worse VF status in younger eyes, but not older eyes. Kim et al.[13] reported the LC depth was significantly correlated with the MD in NTG eyes, but not POAG. In agreement with the results in NTG eyes, our study concluded that the LC was deeper in PXG eyes compared with controls and that the LC depth was associated with disease severity.

Our data showed a significant association between IOP and ALD in PXG after adjustment for confounders. Previous animal studies reported posterior displacement of the LC at increasing IOP.[47] Using EDI in POAG eyes, Kim et al.[46] found a significant association of LC depth with baseline IOP, but not IOP at the time of study examination. Even though many of our patients were under intensive IOP-lowering management, a link between IOP at presentation and the LC depth was detected. This discrepancy might be due to the relative irreversibility of LC displacement secondary to specific characteristics of PXG eyes, which have been shown in experimental animal models.[14] We also did not find any significant difference in LC depth between PXS and control eyes, suggesting that LC thinning might occur before LC deepening.

In the present study, LC depth was measured relative to the anterior scleral surface. Previous studies have used the BMO as a reference plane. However, recent cross-sectional studies have shown that BMO is not a stable reference due to significant thinning of the choroid and posterior migration of the BMO

with aging.[20,21] Alternatively, the anterior scleral surface has been found as a reference that could eliminate the influence of choroidal thickness.[36,48] This definition was necessary to avoid bias in our study, as choroidal thickness was thinner in more advanced stages of PXG.

Previous studies evaluating the choroidal thickness in glaucomatous eyes as a marker of choroidal blood flow have reported conflicting results.[15–21] In a meta-analysis of 22 studies, Zhang et al.[21] suggested that POAG was not significantly associated with a marked thinning or thickening of the choroid based on EDI-OCT measurements. Nevertheless, the type of glaucoma may affect choroidal thickness. In the present study, the choroidal thickness was comparable among mild PXG, PXS, and controls. There are various studies investigating whether retrobulbar hemodynamics change in PXG.[50,51] Galassi et al.[50] determined that retrobulbar hemodynamics were impaired in PXG compared with POAG and healthy controls, which the investigators interpreted as the presence of impaired ocular vascular regulation in PXG. Turan-Vural et al.[28] reported decreased subfoveal choroidal thickness in nonglaucomatous PXS eyes compared with healthy controls. In contrast, Moghimi et al.[12,30] did not show any difference in peripaillary and macular choroidal thickness in PXS eyes compared with controls after adjusting for age and axial length. Likewise, You et al.[52] reported that PXS was not associated with the choroidal thickness in the Beijing Eye Study 2011.

Although Ozge et al.[29] demonstrated that peripapillary choroidal thickness was comparable in PXG eyes and healthy controls, another recent study found choroidal thickness to be thinner in the nasal quadrant of macula in PXG eyes.[15] Similarly, Dursun et al.[16] compared the choroidal thickness of 30 PXS eyes, 28 PXG eyes, and 30 age-matched healthy eyes and found a nonstatistically significant thinner choroid in PXG compared with PXS. However, all these studies analyzed patients affected by early or moderate glaucoma, with an average MD always better than −12 dB. In the present study, we showed that moderate to advanced PXG eyes had thinner choroid when compared with mild PXG, PXS, and healthy controls. This observation suggests that choroidal thickness occurs later in the disease course of pseudoexfoliation and that factors other than choroidal thinning may play a role in the conversion from PXS to PXG. Sacconi and associates[24] have also reported choroidal thinning in advanced POAG. Nevertheless, due to limited information on the relationship between choroidal blood flow and choroidal thickness in humans, we are unable to conclude based on our results whether choroidal blood flow was normal in eyes with early stages of pseudoexfoliation despite having choroidal thickness within the normal range.

Although many investigators have shown significant links between demographics, ocular parameters, and choroidal thickness in healthy and POAG eyes, no study has evaluated factors related to choroidal thicknesses in patients with PXG. Roberts and associates[23] found that choroidal thickness was inversely associated with age and axial length. Similarly, Mwanza and associates[20] found a similar association of age with axial length, but not with IOP or blood pressure. Conversely, in a study on PXS eyes, Moghimi et al.[12] showed no links between choroidal thickness and age, axial length, and CCT. In the present study, glaucoma severity was the only factor that correlated with choroidal thickness in PXG eyes. Although the MD was not correlated with choroidal thickness in POAG eyes,[25] one recent study showed choroidal thinning in advanced POAG[24] and concluded that the longer duration of glaucoma may lead to ocular changes like vascular impairment and diffuse loss of choroidal vessels.

Several limitations must be acknowledged in this study. As we defined the PXS group to have normal IOP, some of the differences between the PXG eyes and controls may be underestimated. This is especially true for ALD, as it has been well-described that IOP can alter this parameter.[10,33,53] The operating software of the Heidelberg Spectralis OCT did not provide automatic segmentation of the choroid and LC. Manual segmentation may introduce some inaccuracy, although the intraobserver and interobserver ICCs all were more than 0.99 for choroid and 0.83 for LC parameters in this study. While EDI substantially improved the image quality of the LC, it was still difficult to determine the border of the LC in some images (16% of PXG, 27% of PXS, and 29% of controls). Thus, our analysis was limited to eyes demonstrating a clear border of LC, which may have biased the results similar to other LC imaging studies using EDI technology. A recent study using a single line scan on three OCT devices showed that the anterior LC was the most detectable feature, followed by the LC insertions and then the posterior boundary; and that LC visibility was not affected by glaucoma severity.[36] However, several cohorts evaluated LC thickness and posterior boundary in different eye diseases and used the EDI three-dimensional raster scan pattern to improve detection.[13,32,33,42] In this method, it is possible to view multiple successive B scans within a volume to look for consistent visual clues that may help to identify the posterior laminar surface. We used the same protocol to detect the LC surfaces of the study cases with improved precision.

Most of the PXG eyes were under intensive IOP-lowering therapy and the information about baseline IOP was not available. Therefore, the relationship between baseline IOP (untreated IOP) and OCT parameters could not be evaluated. Finally, it is not possible to determine the cause-effect relationship between LC and choroidal characteristics and disease severity because of the cross-sectional nature of the study and the lack of POAG eyes as a comparison group. One could argue that these changes in the choroid and ONH may occur in any glaucomatous process and might not be specific to pseudoexfoliation. Further prospective, longitudinal study is warranted.

To summarize, LC thinning occurs early in pseudoexfoliation and its extent is linked to glaucoma severity. Although LC posterior displacement was associated with diagnosis of glaucoma and severity, choroidal thinning may not be detected until late in the disease course.

Acknowledgments

The authors thank Nassim Khatibi for her assistance in data collection. All authors attest that they meet the current International Committee of Medical Journal Editors criteria for authorship.

Supported in part by National Institutes of Health/National Eye Institute Grant R01EY029058 and an unrestricted grant from Research to Prevent Blindness (New York, NY, USA).

Disclosure: **S. Moghimi**, None; **S. Nekoozadeh**, None; **N. Motamed-Gorji**, None; **R. Chen**, None; **M.A. Fard**, None; **M. Mohammadi**, None; **R.N. Weinreb**, Carl Zeiss Meditec (F), Genentech (F), Heidelberg Engineering (F), National Eye Institute (F), Optovue (F), Tomey (F), Aerie Pharmaceutical (F), Alcon (F), Allergan (F), Bausch & Lomb (F), Eyenovia (F), Novartis (F), Unity (F)

References

1. Ritch R, Schlötzer-Schrehardt U. Exfoliation syndrome. *Surv Ophthalmol*. 2001;45:265–315.
2. Recupero SM, Contestabile MT, Taverniti L, et al. Open-angle glaucoma: variations in the intraocular pressure after visual field examination. *J Glaucoma*. 2003;12:114–148.

3. Grodum K, Heijl A, Bengtsson B. Risk of glaucoma in ocular hypertension with and without pseudoexfoliation. *Ophthalmology*. 2005;112:386–390.
4. Plateroti P, Plateroti AM, Abdolrahimzadeh S, Scuderi G. Pseudoexfoliation syndrome and pseudoexfoliation glaucoma: a review of the literature with updates on surgical management. *J Ophthalmol*. 2015;2015:370371.
5. Leske MC, Heijl A, Hyman L, et al. Predictors of long-term progression in the early manifest glaucoma trial. *Ophthalmology*. 2007;114:1965–1972.
6. Netland PA, Ye H, Streeten BW, Hernandez MR. Elastosis of the lamina cribrosa in pseudoexfoliation syndrome with glaucoma. *Ophthalmology*. 1995;102:878–886.
7. Schlötzer-Schrehardt U, Hammer CM, Krysta AW, et al. LOXL1 deficiency in the lamina cribrosa as candidate susceptibility factor for a pseudoexfoliation-specific risk of glaucoma. *Ophthalmology*. 2012;119:1832–1843.
8. Pena JD, Netland PA, Vidal I, et al. Elastosis of the lamina cribrosa in glaucomatous optic neuropathy. *Exp Eye Res*. 1998;67:517–524.
9. Bellezza AJ, Rintalan CJ, Thompson HW, et al. Deformation of the lamina cribrosa and anterior scleral canal wall in early experimental glaucoma. *Invest Ophthalmol Vis Sci*. 2003;44:623–637.
10. Park SC, Brumm J, Furlanetto RL, et al. Lamina cribrosa depth in different stages of glaucoma. *Invest Ophthalmol Vis Sci*. 2015;56:2059–2064.
11. Quigley HA, Addicks EM, Green WR, Maumenee AE. Optic nerve damage in human glaucoma. II. The site of injury and susceptibility to damage. *Arch Ophthalmol*. 1981;99:635–649.
12. Moghimi S, Mazloumi M, Johari M, et al. Evaluation of lamina cribrosa and choroid in nonglaucomatous patients with pseudoexfoliation syndrome using spectral-domain optical coherence tomography. *Invest Ophthalmol Vis Sci*. 2016;57:1293–1300.
13. Kim S, Sung KR, Lee JR, Lee KS. Evaluation of lamina cribrosa in pseudoexfoliation syndrome using spectral-domain optical coherence tomography enhanced depth imaging. *Ophthalmology*. 2013;120:1798–1803.
14. Braunsmann C, Hammer CM, Rheinlaender J, et al. Evaluation of lamina cribrosa and peripapillary sclera stiffness in pseudoexfoliation and normal eyes by atomic force microscopy. *Invest Ophthalmol Vis Sci*. 2012;53:2960–2967.
15. Bayhan HA, Bayhan SA, Can I. Evaluation of the macular choroidal thickness using spectral optical coherence tomography in pseudoexfoliation glaucoma. *J Glaucoma*. 2016;25:184–187.
16. Dursun A, Ozec AV, Dogan O, et al. Evaluation of choroidal thickness in patients with pseudoexfoliation syndrome and pseudoexfoliation glaucoma. *J Ophthalmol*. 2016;2016:3545180.
17. Ehrlich JR, Peterson J, Parlitsis G, et al. Peripapillary choroidal thickness in glaucoma measured with optical coherence tomography. *Exp Eye Res*. 2011;92:189–194.
18. Li L, Bian A, Zhou Q, Mao J. Peripapillary choroidal thickness in both eyes of glaucoma patients with unilateral visual field loss. *Am J Ophthalmol*. 2013;156:1277–1284.e1.
19. Maul EA, Friedman DS, Chang DS, et al. Choroidal thickness measured by spectral domain optical coherence tomography: factors affecting thickness in glaucoma patients. *Ophthalmology*. 2011;118:1571–1579.
20. Mwanza JC, Sayyad FE, Budenz DL. Choroidal thickness in unilateral advanced glaucoma. *Invest Ophthalmol Vis Sci*. 2012;53:6695–6701.
21. Zhang Z, Yu M, Wang F, et al. Choroidal thickness and open-angle glaucoma: a meta-analysis and systematic review. *J Glaucoma*. 2016;25:e446–e454.
22. Hayreh SS. Blood supply of the optic nerve head and its role in optic atrophy, glaucoma, and oedema of the optic disc. *Br J Ophthalmol*. 1969;53:721–748.
23. Roberts KF, Artes PH, O'Leary N, et al. Peripapillary choroidal thickness in healthy controls and patients with focal, diffuse, and sclerotic glaucomatous optic disc damage. *Arch Ophthalmol*. 2012;130:980–986.
24. Sacconi R, Deotto N, Merz T, et al. SD-OCT choroidal thickness in advanced primary open-angle glaucoma. *J Glaucoma*. 2017;26:523–527.
25. Hosseini H, Nilforushan N, Moghimi S, et al. Peripapillary and macular choroidal thickness in glaucoma. *J Ophthalmic Vis Res*. 2014;9:154–161.
26. Goktas S, Sakarya Y, Ozcimen M, et al. Choroidal thinning in pseudoexfoliation syndrome detected by enhanced depth imaging optical coherence tomography. *Eur J Ophthalmol*. 2014;24:879–884.
27. Eroglu FC, Asena L, Simsek C, et al. Evaluation of choroidal thickness using enhanced depth imaging by spectral-domain optical coherence tomography in patients with pseudoexfoliation syndrome. *Eye (Lond)*. 2015;29:791–796.
28. Turan-Vural E, Yenerel N, Okutucu M, et al. Measurement of subfoveal choroidal thickness in pseudoexfoliation syndrome using enhanced depth imaging optical coherence tomography. *Ophthalmologica*. 2015;233:204–208.
29. Ozge G, Koylu MT, Mumcuoglu T, et al. Evaluation of retinal nerve fiber layer thickness and choroidal thickness in pseudoexfoliative glaucoma and pseudoexfoliative syndrome. *Postgrad Med*. 2016;128:444–448.
30. Moghimi S, Mazloumi M, Johari MK, et al. Comparison of macular choroidal thickness in patients with pseudoexfoliation syndrome to normal control subjects with enhanced depth SD-OCT imaging. *J Curr Ophthalmol*. 2017;29:258–263.
31. Kagemann L, Ishikawa H, Wollstein G, et al. Ultrahigh-resolution spectral domain optical coherence tomography imaging of the lamina cribrosa. *Ophthalmic Surg Lasers Imaging*. 2008;39(4 Suppl):S126–S131.
32. Jonas JB, Berenshtein E, Holbach L. Lamina cribrosa thickness and spatial relationships between intraocular space and cerebrospinal fluid space in highly myopic eyes. *Invest Ophthalmol Vis Sci*. 2004;45:2660–2665.
33. Kim M, Bojikian KD, Slabaugh MA, et al. Lamina depth and thickness correlate with glaucoma severity. *Indian J Ophthalmol*. 2016;64:358–363.
34. Johnson CA, Sample PA, Cioffi GA, et al. Structure and function evaluation (SAFE): I. criteria for glaucomatous visual field loss using standard automated perimetry (SAP) and short wavelength automated perimetry (SWAP). *Am J Ophthalmol*. 2002;134:177–185.
35. Spaide RF, Koizumi H, Pozonni MC. Enhanced depth imaging spectral-domain optical coherence tomography. *Am J Ophthalmol*. 2008;146:496–500.
36. Johnstone J, Fazio M, Rojananuangnit K, et al. Variation of the axial location of Bruch's membrane opening with age, choroidal thickness, and race. *Invest Ophthalmol Vis Sci*. 2014;55:2004–2009.
37. Lee EJ, Kim TW, Weinreb RN. Reversal of lamina cribrosa displacement and thickness after trabeculectomy in glaucoma. *Ophthalmology*. 2012;119:1359–1366.
38. Leung CK, Ye C, Weinreb RN, et al. Retinal nerve fiber layer imaging with spectral-domain optical coherence tomography: a study on diagnostic agreement with Heidelberg Retinal Tomograph. *Ophthalmology*. 2010;117:267–274.
39. Enderlein G, Fleiss JL. *The Design and Analysis of Clinical Experiments*. New York, NY: Wiley; 1986.
40. Park HY, Jeon SH, Park CK. Enhanced depth imaging detects lamina cribrosa thickness differences in normal tension

Investigative Ophthalmology & Visual Science

glaucoma and primary open-angle glaucoma. *Ophthalmology*. 2012;119:10–20.

41. Hammer T, Schlotzer-Schrehardt U, Naumann GO. Unilateral or asymmetric pseudoexfoliation syndrome? An ultrastructural study. *Arch Ophthalmol*. 2001;119:1023–1031.
42. Lee EJ, Kim TW, Kim M, Kim H. Influence of lamina cribrosa thickness and depth on the rate of progressive retinal nerve fiber layer thinning. *Ophthalmology*. 2015;122:721–729.
43. Gaasterland D, Tanishima T, Kuwabara T. Axoplasmic flow during chronic experimental glaucoma. 1. Light and electron microscopic studies of the monkey optic nervehead during development of glaucomatous cupping. *Invest Ophthalmol Vis Sci*. 1978;17:838–846.
44. Burgoyne CF, Downs JC. Premise and prediction–how optic nerve head biomechanics underlies the susceptibility and clinical behavior of the aged optic nerve head. *J Glaucoma*. 2008;17:318.
45. Ren R, Yang H, Gardiner SK, et al. Anterior lamina cribrosa surface depth, age, and visual field sensitivity in the Portland Progression Project. *Invest Ophthalmol Vis Sci*. 2014;55:1531–1539.
46. Kim YW, Kim DW, Jeoung JW, et al. Peripheral lamina cribrosa depth in primary open-angle glaucoma: a swept-source optical coherence tomography study of lamina cribrosa. *Eye (Lond)*. 2015;29:1368–1374.
47. Yang H, Williams G, Downs JC, et al. Posterior (outward) migration of the lamina cribrosa and early cupping in monkey experimental glaucoma. *Invest Ophthalmol Vis Sci*. 2011;52:7109–7121.
48. Sawada Y, Hangai M, Murata K, et al. Lamina cribrosa depth variation measured by spectral-domain optical coherence tomography within and between four glaucomatous optic disc phenotypes. *Invest Ophthalmol Vis Sci*. 2015;56:5777–5784.
49. Quigley HA, Hohman RM, Addicks EM, et al. Morphologic changes in the lamina cribrosa correlated with neural loss in open-angle glaucoma. *Am J Ophthalmol*. 1983;95:673–691.
50. Galassi F, Giambene B, Menchini U. Ocular perfusion pressure and retrobulbar haemodynamics in pseudoexfoliative glaucoma. *Graefes Arch Clin Exp Ophthalmol*. 2008;246:411–416.
51. Schlötzer-Schrehardt U, von der Mark K, Sakai LY, Naumann GO. Increased extracellular deposition of fibrillin-containing fibrils in pseudoexfoliation syndrome. *Invest Ophthalmol Vis Sci*. 1997;38:970–984.
52. You QS, Xu L, Wang YX, et al. Pseudoexfoliation: normative data and associations: the Beijing eye study 2011. *Ophthalmology*. 2013;120:1551–1558.
53. Lee EJ, Kim TW, Weinreb RN. Variation of lamina cribrosa depth following trabeculectomy. *Invest Ophthalmol Vis Sci*. 2013;54:5392–5399.

Investigative Ophthalmology & Visual Science